

Supplementary material for Lagrangian investigation into the representation of aerosol size distribution in climate models during the 2014-15 Holuhraun eruption.

Table of Contents

<i>S1 Supplementary Methods</i>	2
S1.1 Data references.....	2
S1.2 Particle number size distribution data filters.....	3
S1.3 GCM aerosol modes.....	5
S1.4 Trajectory start heights.....	6
S1.5 Clustering	6
<i>S2 Supplementary Results</i>	7
S2.1 Aerosol size distribution time series.....	7
S2.2 NMBF results	10
S2.3 Perturbation of aerosol size distribution compared to climatology	11
S2.4 Transport.....	13
S2.5 Potential impact on cloud microphysics	14

S1 Supplementary Methods

S1.1 Data references

Pallas (Matorova)	September 2014	Makkonen, U. EMEP, 2013-2015, Inorganics in air and particle phase at Pallas (Matorova), data hosted by EBAS at NILU, DOI: https://doi.org/10.48597/PPB3-N5YU
Zeppelin (Ny-Ålesund)	September 2014	From personal correspondence with Ove Hermansen at NILU (Norwegian Institute for Air Research)

Table S1: References for the SO₂ measurements.

Värriö	2009-2014	Kulmala, M., Aalto, P., ACTRIS, GAW-WDCA, EMEP, 2000-2016, Particle_number_size_distribution at Värriö, data hosted by EBAS at NILU, DOI: https://doi.org/10.48597/GCM5-XUH5
Pallas (Sammaltunturi)	2009-2014	Kivekäs, N. GAW-WDCA, EUSAAR, EMEP, ACTRIS, CREATE, 2008-2011, Particle_number_size_distribution at Pallas (Sammaltunturi), data hosted by EBAS at NILU, DOI: https://doi.org/10.48597/DS2W-2XKG
	2012-2014	Kivekäs, N., Seppälä, S., Hyvärinen, A. GAW-WDCA, ACTRIS, EMEP, 2012-2021, Particle_number_size_distribution at Pallas (Sammaltunturi), data hosted by EBAS at NILU, DOI: https://doi.org/10.48597/5PPZ-42F4
Zeppelin (Mountain)	2010-2014	Tunved, P. ACTRIS, GAW-WDCA, 2010-2021, Particle_number_size_distribution at Zeppelin Mountain (Ny-Ålesund), data hosted by EBAS at NILU, DOI: https://doi.org/10.48597/REFE-7BYF

Table S2: References for the ACTRIS PNSD measurements.

S1.2 Particle number size distribution data filters

Filter removal rates for each yearly aerosol file are shown for Värriö in Table S3, Pallas in Table S4 and Zeppelin in Table S5.

Year	Datapoints at start	Percentage of empty distributions at start	Percentage points removed for 1	Percentage points removed for 2	Percentage points removed for 3	Percentage points removed for 4
2009	8760	27.52	2.37	0	0.20	0.5
2010	8760	75.32	0	0	0.00	0.5
2011	8760	2.5	22.8	0	0.66	0.5
2012	8784	1.04	4.08	0	0.40	0.5
2013	8760	1.39	5.77	0	0.21	0.5
2014	8760	3.54	0	0	0.56	0.5

Table S3: The percentage of datapoints removed from each yearly aerosol file by each filter for Värriö. Filtering conducted on the full timeseries from 2009-2014.

Year	Datapoints at start	Percentage of empty distributions at start	Percentage points removed for 1	Percentage points removed for 2	Percentage points removed for 3	Percentage points removed for 4
2009	8760	44.71	0	0	0.18	0.5
2010	8760	38.36	0	0	0.41	0.5
2011	8760	51.28	0	0	0.55	0.5
2012	8784	99.36	0	0	0.00	0.5
2013	8760	40.70	0	0	0.67	0.5
2014	8760	39.57	0	0	1.19	0.5

Table S4: The percentage of datapoints removed from each yearly aerosol file by each filter for Pallas. Filtering conducted on statistics from the full timeseries 2009-2014.

Year	Datapoints at start	Number of empty distributions at start	Percentage points removed for 1	Percentage points removed for 2	Percentage points removed for 3	Percentage points removed for 4
2010	8760	70.23	0	0	0.02	0.5
2011	8760	43.63	0	0	0.40	0.5
2012	8784	13.31	0	0	1.05	0.5
2013	8760	11.53	0	0	0.38	0.5
2014	8760	49.63	0	0	0.10	0.5

Table S5: The percentage of datapoints removed from each yearly aerosol file by each filter for Zeppelin. Filtering conducted on statistics from the full timeseries 2010-2014.

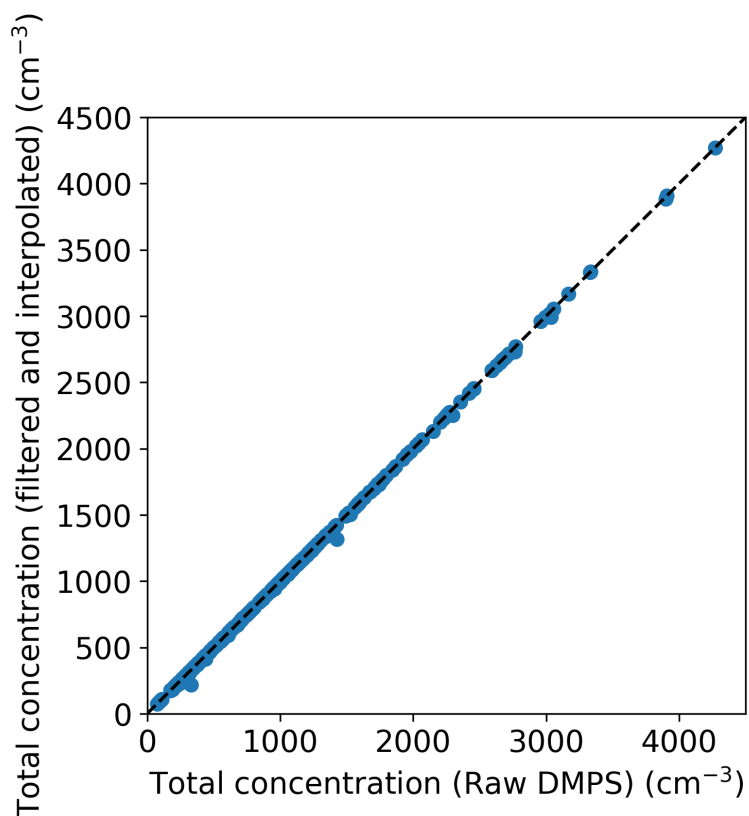


Figure S1: Total concentration for September 2014 at Värriö for the raw DMPS measurements compared to the filtered and interpolated PNSD.

S1.3 GCM aerosol modes

Aerosol mode	Species	Diameter (nm)	Geometric standard deviation (σ)
Nucleation soluble	SO ₄ , OM	1–10	1.59
Aitken soluble	SO ₄ , BC, OM	10–100	1.59
Accumulation soluble	SO ₄ , BC, OM, SS	100–500	1.40
Coarse soluble	SO ₄ , BC, OM, SS	500–10000	2.00
Aitken insoluble	BC, OM	10–100	1.59

Table S6: UKESM1.0 aerosol mode descriptions. Species comprise sulphate (SO₄), organic matter (OM), black carbon (BC) and sea salt (SS).

Aerosol mode	Species	Diameter (nm)	Geometric standard deviation (σ)
Nucleation soluble	SO ₄ ,	< 10	1.59
Aitken soluble	SO ₄ , OC, BC	10–100	1.59
Accumulation soluble	SO ₄ , OC, BC, SS	100–1000	1.59
Coarse soluble	SO ₄ , OC, BC, SS	>1000	2.00
Aitken insoluble	OC, BC	10–100	1.59
Accumulation insoluble	Dust	100–1000	1.59
Coarse insoluble	Dust	>1000	2.00

Table S7: ECHAM6.3-HAM2.3 aerosol mode descriptions. Components are as in Table 2.1, but OC here is used to represent organic matter rather than organic carbon (OC).

S1.4 Trajectory start heights

Station	Altitude (m a.s.l.)	ERA-Int difference	UKESM difference	ECHAM difference	Average offset	Height above ground level used (to the nearest 50m)
VAR	390	142.9	180.4	142.7	155.6	150
PAL	565	269.7	192.9	191.8	218.1	200
ZEP	472	288.6	333.8	362.9	328.4	350

Table S8: Altitude of station compared to the orography at that point for each dataset (ERA-Interim, UKESM1.0, ECHAM6.3-HAM2.3). The mean of the offsets between the datasets is then used to select the height above ground level used (to the nearest 50m).

S1.5 Clustering

The ‘Elbow’ method was employed to select the number of clusters based on the decrease of within-cluster sum of squares (WCSS).

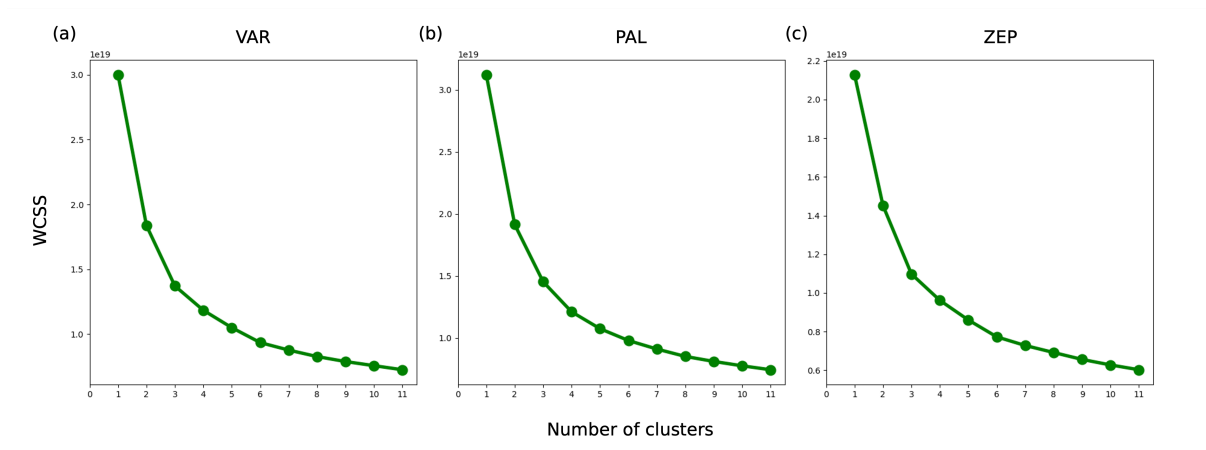


Figure S2: The within-cluster sum of squares (WCSS) for each number of clusters from 1-11 for each station (a) Värriö, (b) Pallas and (c) Zeppelin.

S2 Supplementary Results

S2.1 Aerosol size distribution time series

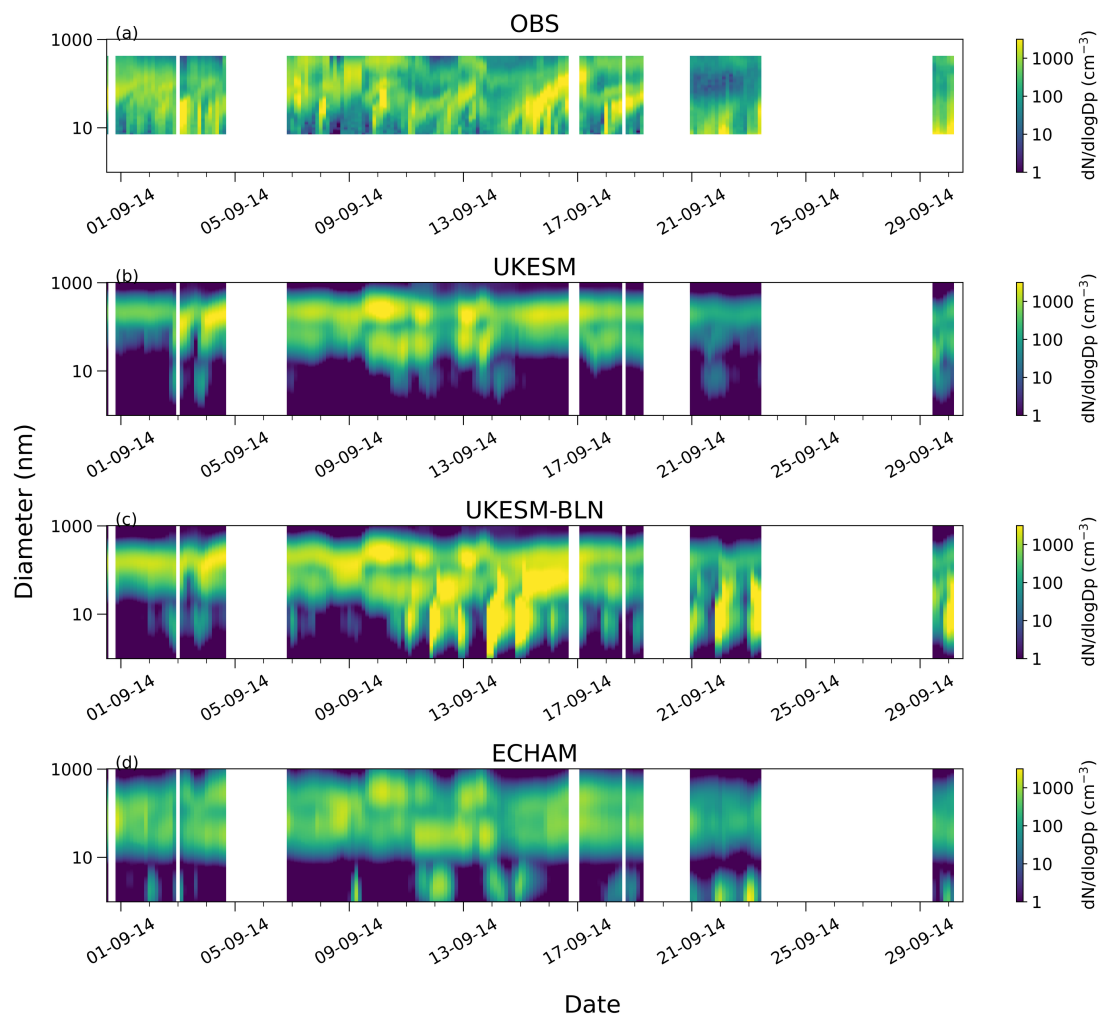


Figure S3: Timeseries of size distribution for September 2014 at Pallas in $dN/d\log D_p$. (a) observations (DMPS), (b) UKESM1.0, (c) UKESM1.0-BLN and (d) ECHAM6.3HAM2.3.

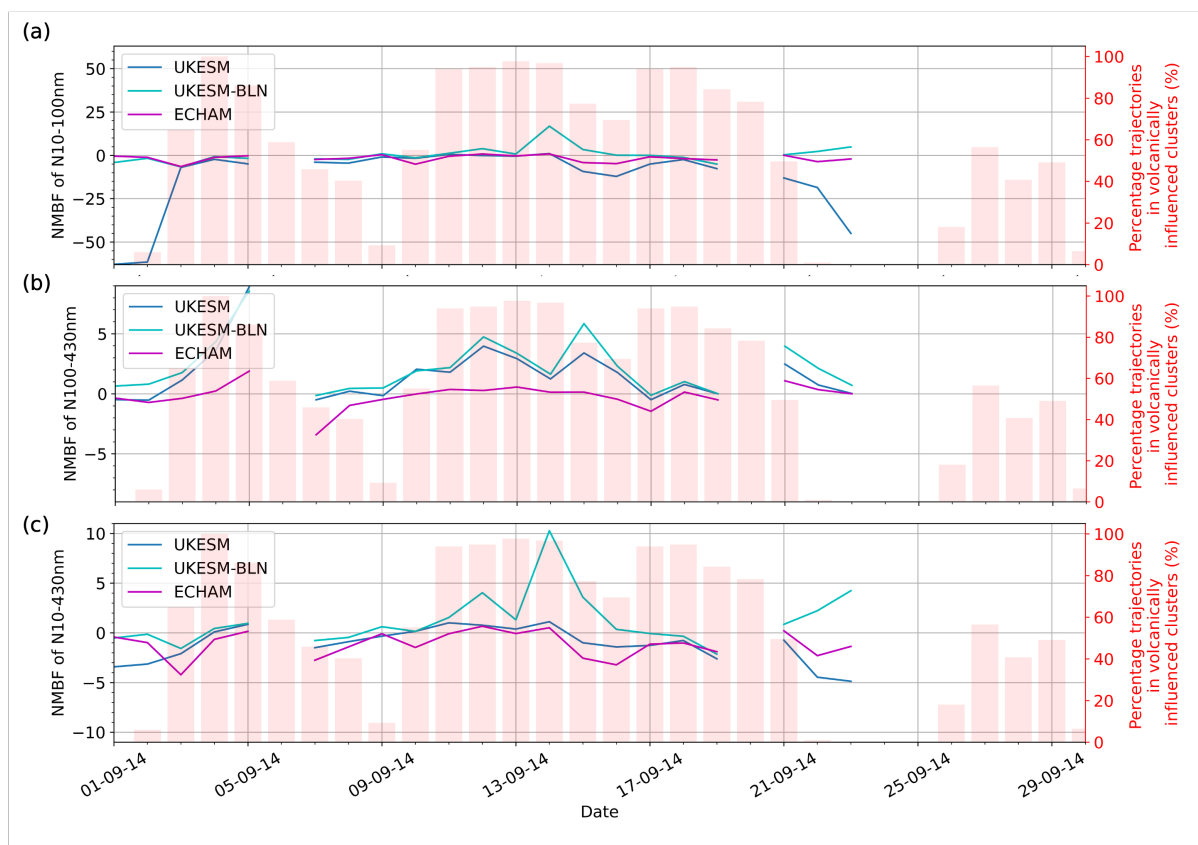


Figure S4: Timeseries of normalised mean bias factor (NMBF) (Eq. 4) per day during September 2014 at Pallas for the for different size ranges for each model compared to observations: (a) Aitken mode (10-100nm) (b) accumulation mode (100-430nm) and (c) total (10-430nm). UKESM1.0 is shown in blue, UKESM1.0-BLN in cyan and ECHAM6.3-HAM2.3 in magenta. The period which was found to be influenced by transport from the volcano from the clustering analysis (Sect. 2.7) is indicated by the red shading of the timeseries.

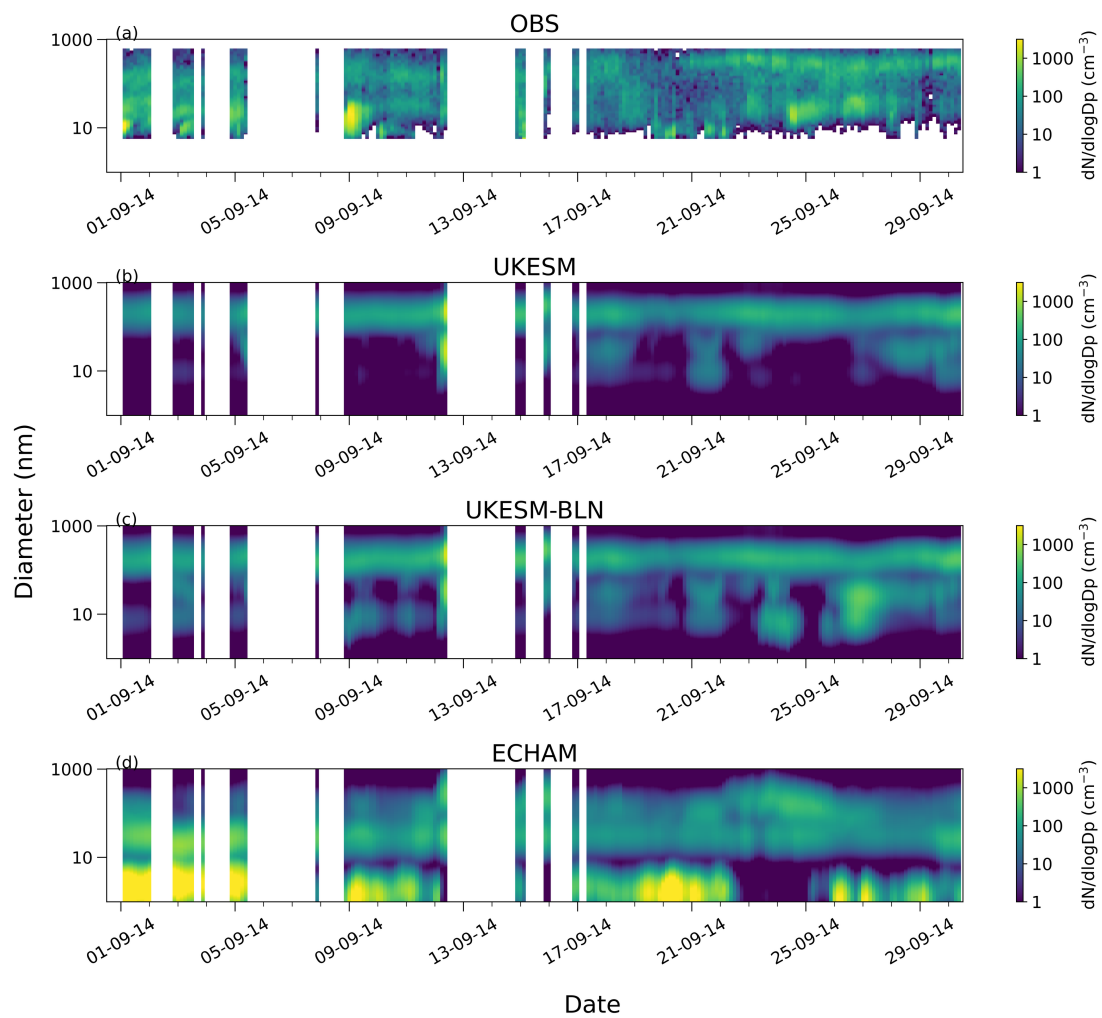


Figure S5: Timeseries of size distribution for September 2014 at Zeppelin in $dN/d\log D_p$. (a) observations (DMPS), (b) UKESM1.0, (c) UKESM1.0-BLN and (d) ECHAM6.3HAM2.3.

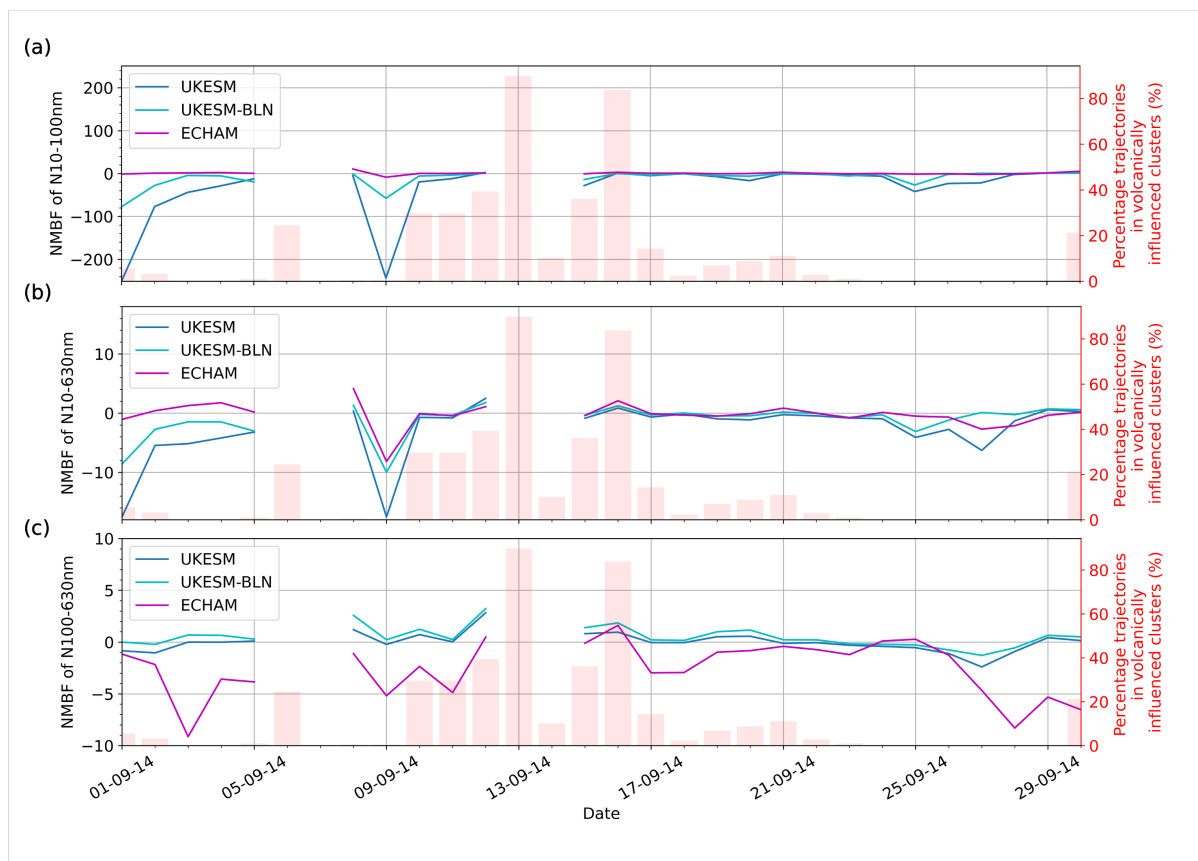


Figure S6: Timeseries of normalised mean bias factor (NMBF) (Eq. 4) per day during September 2014 at Zeppelin for the concentration for different size ranges for each model compared to observations: (a) Aitken mode (10-100nm) (b) accumulation mode (100-630nm) and (c) total (10-630nm). UKESM1.0 is shown in blue, UKESM1.0-BLN in cyan and ECHAM6.3-HAM2.3 in magenta. The period which was found to be influenced by transport from the volcano from the clustering analysis (Sect. 2.7) is indicated by the red shading of the timeseries.

S2.2 NMBF results

	Värriö (N10-790nm)	Pallas (N10-430nm)	Zeppelin (N10-630nm)
UKESM	-0.67 1.67 (underestimation)	-0.46 1.46 (underestimation)	-1.24 2.24 (underestimation)
UKESM-BLN	0.98 1.98 (overestimation)	0.69 1.69 (overestimation)	-0.60 1.60 (underestimation)
ECHAM	-0.77 1.77 (underestimation)	-0.97 1.97 (underestimation)	-0.28 1.28 (underestimation)

Table S9: The normalised mean bias factor (NMBF) and model bias factor ($1+|NMBF|$), demonstrating the factor by which each model overestimates or underestimates the total concentration compared to the observations during September 2014 at Värriö ($D_p=10-790\text{nm}$), Pallas ($D_p=10-430\text{nm}$) and Zeppelin ($D_p=10-630\text{nm}$).

S2.3 Perturbation of aerosol size distribution compared to climatology

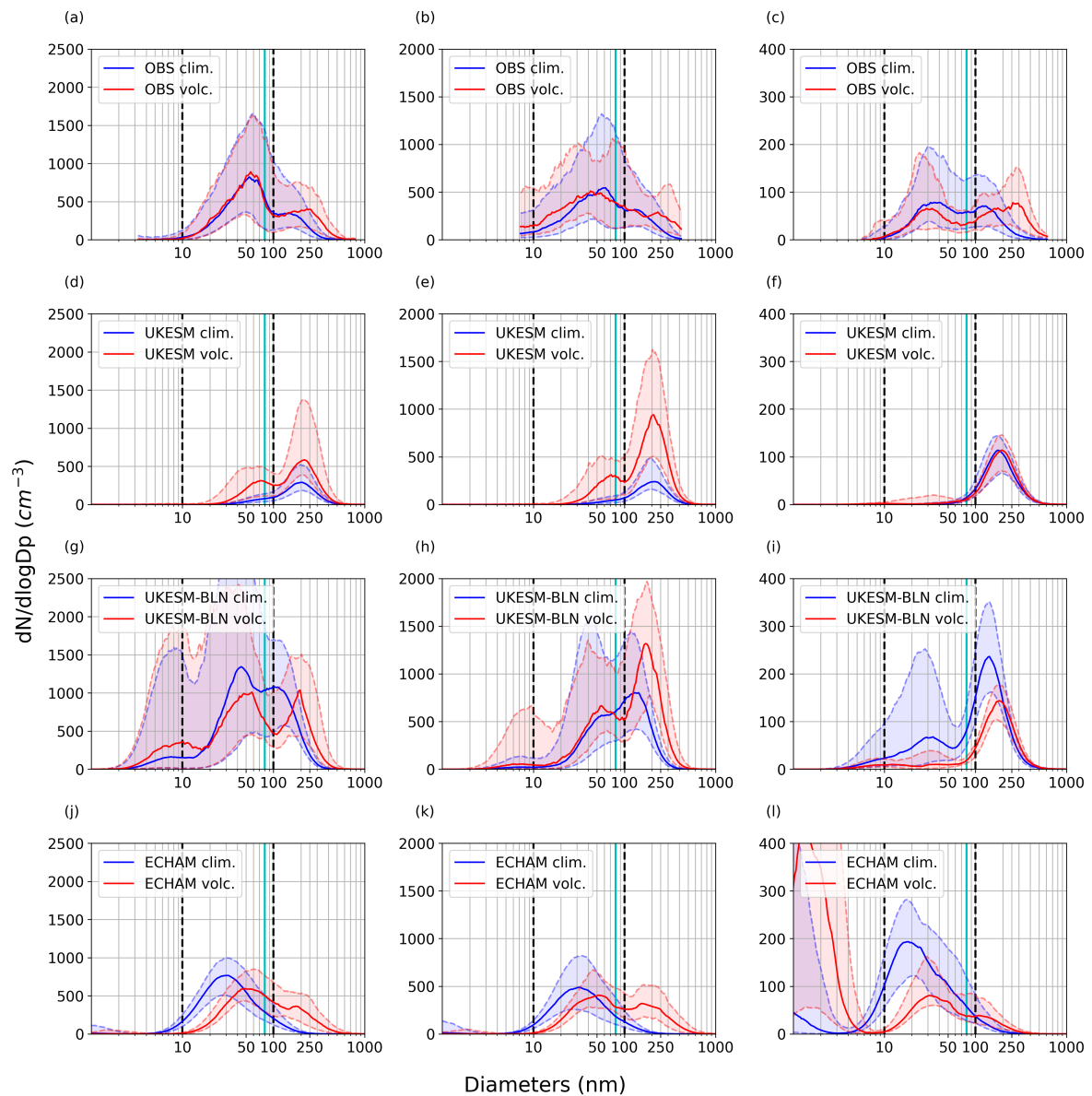


Figure S7: Average size distribution for September at each site. Top panel shows observations (DMPS), middle panel shows UKESM1.0 results and bottom panel shows ECHAM6.3HAM2.3. Red represents the eruption year (2014) and blue the climatology years (Värriö and Pallas: 2009-2013, Zeppelin: 2010-2013). Median indicated by solid line and 25th-75th percentiles by the shaded region.

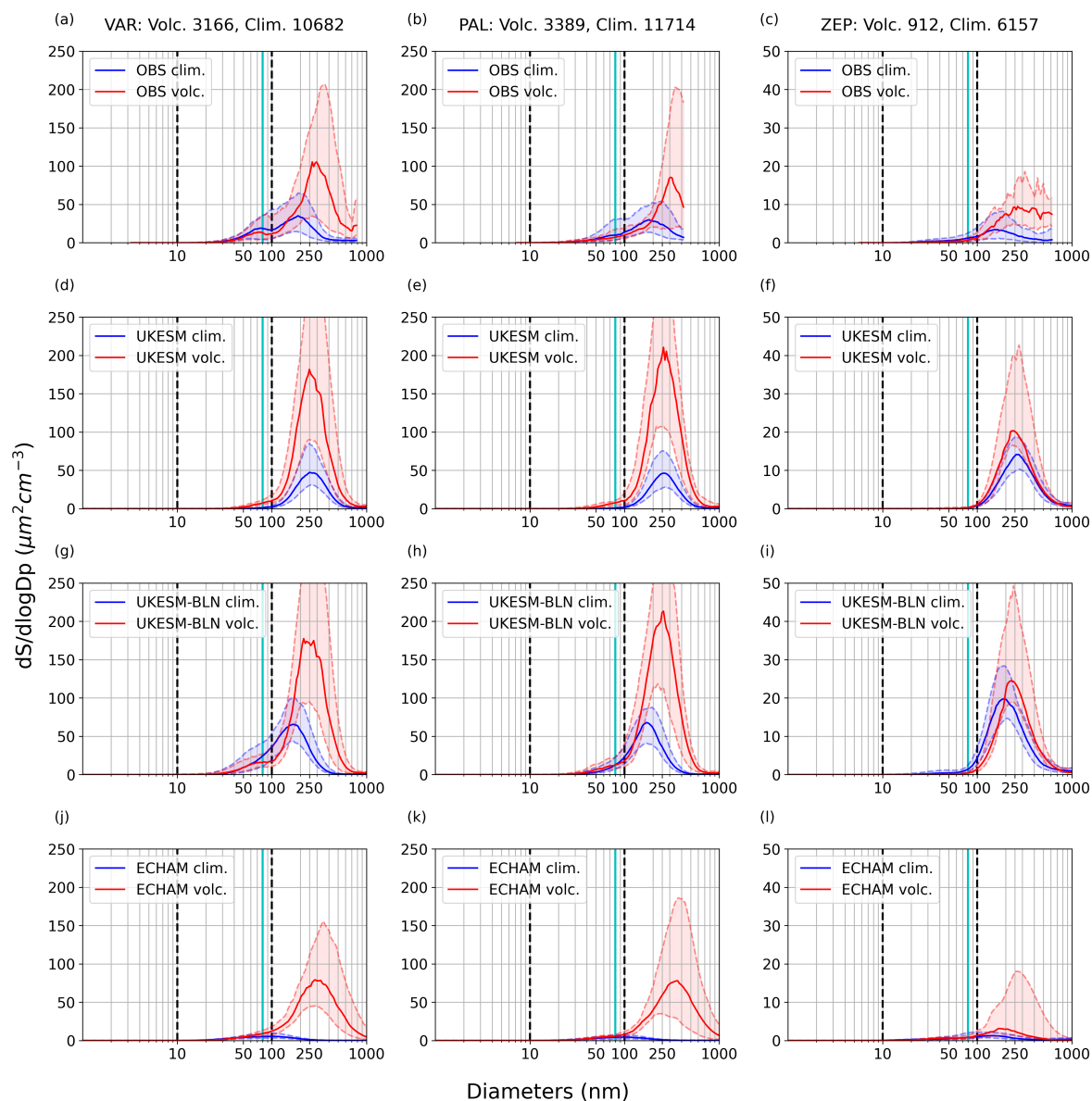


Figure S8: Average surface area ($dS/d\log D_p$) distribution for September at each site. (a-c) Shows observations (DMPS), (d-f) UKESM1.0, (g-i) UKESM1.0-BLN and (j-l) ECHAM6.3-HAM2.3. Red represents the eruption year (2014) and blue the climatology years (Värriö and Pallas: 2009–2013, Zeppelin: 2010–2013). Median indicated by solid line and 25th–75th percentiles by the shaded region. The size distributions are averaged based on data arriving from the direction of Holuhraun, based on the selected clusters in Sect. 2.7. The number of trajectories included in each average is indicated in the title of each column for the climatology and eruption period. The black dotted vertical lines indicate the separation of modes in this study: 1–10 nm to represent the nucleation mode, 10–100 nm to represent the Aitken mode and 100–800 nm to represent the accumulation mode. The cyan vertical lines indicate the 80 nm threshold used as a proxy for CCN in this study.

S2.4 Transport

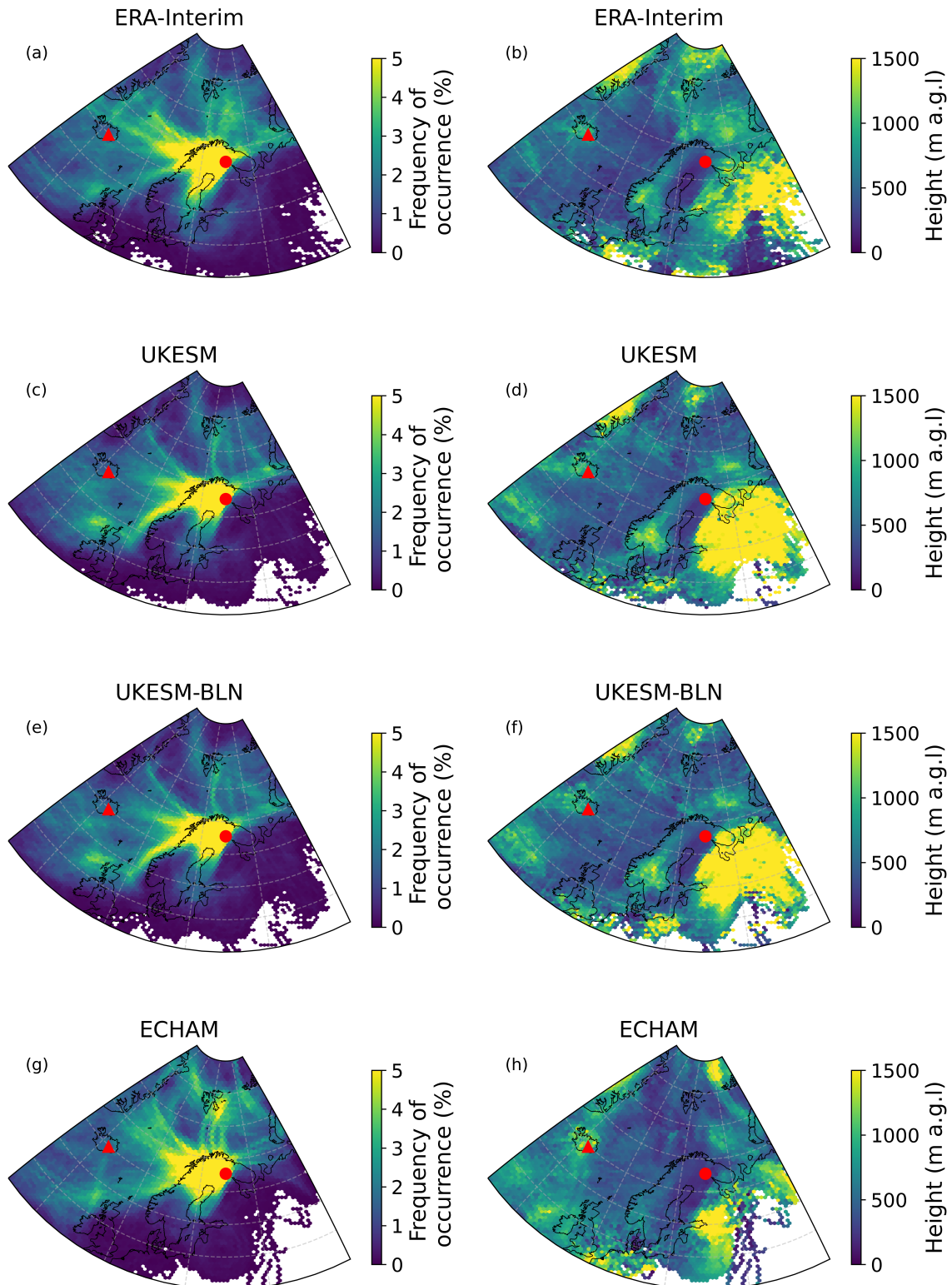


Figure S9: The transport frequency receptor models (a, c, e and g) (Eq. 1) as well as the average height (a.g.l.) (b, d, f and h) for back trajectories passing through a grid cell, calculated using the CVT receptor model (Eq. 3). For all trajectories initialised at Värriö during September 2014, for ERA-Interim (a-b), UKESM1.0 (c-d), UKESM1.0-BLN (e-f) and ECHAM6.3-HAM2.3 (g-h).

S2.5 Potential impact on cloud microphysics

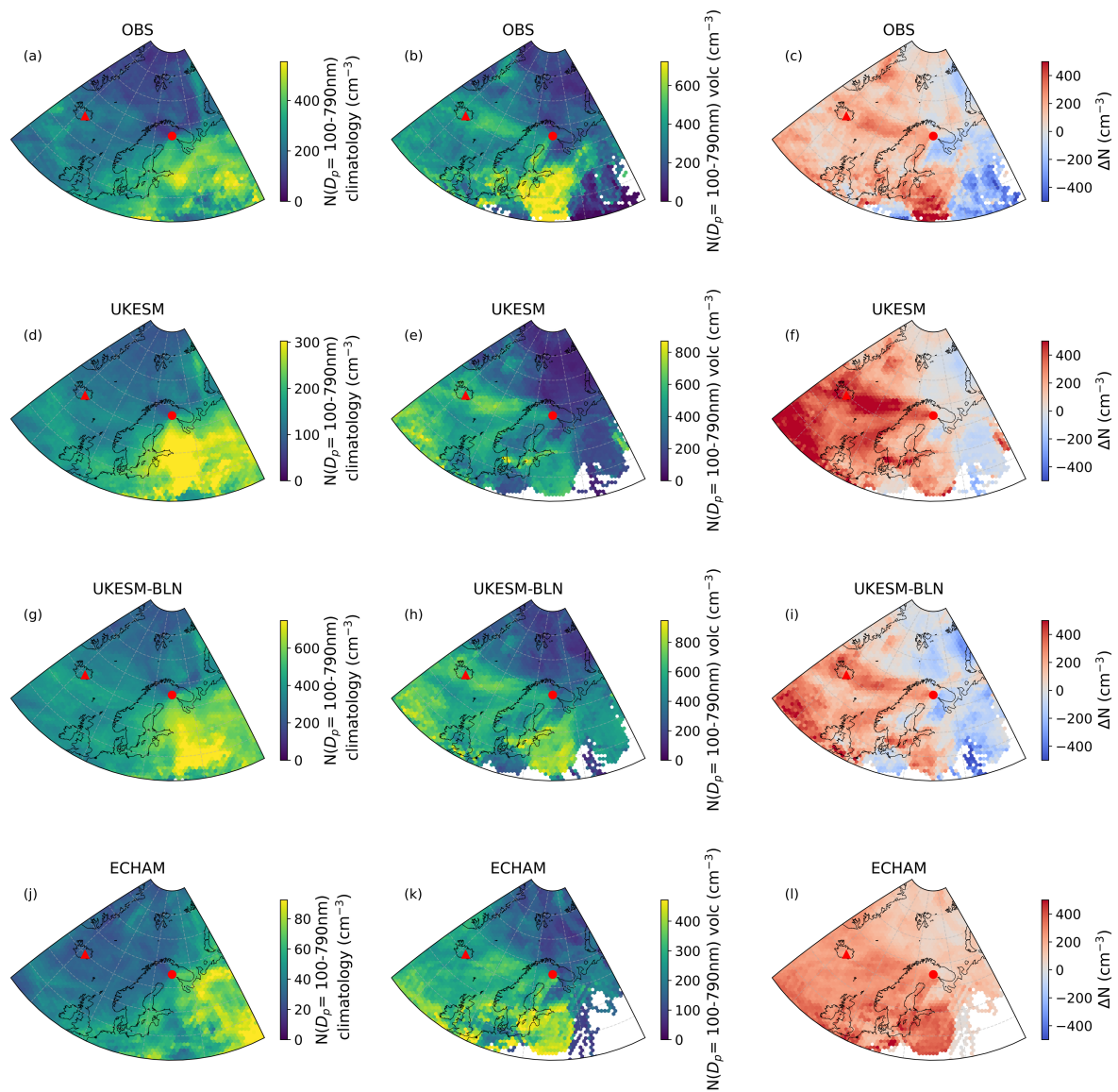


Figure S10: The mean per grid cell for the concentration of particles for $D_p > 100\text{nm}$ (N_{100}) at Värriö for the climatology (a, d, g and j), volcanic period (b, e, h and k) and the difference (volcanic period minus climatology) in concentration (c, f, i and l), utilising the concentration weighted trajectory model. For DMPS with ERA-Interim (a-c), UKESM1.0 (d-f), UKESM1.0-BLN10 (g-i) and ECHAM6.3-HAM2.3 (j-l). Note the difference in colour scale between subfigures.

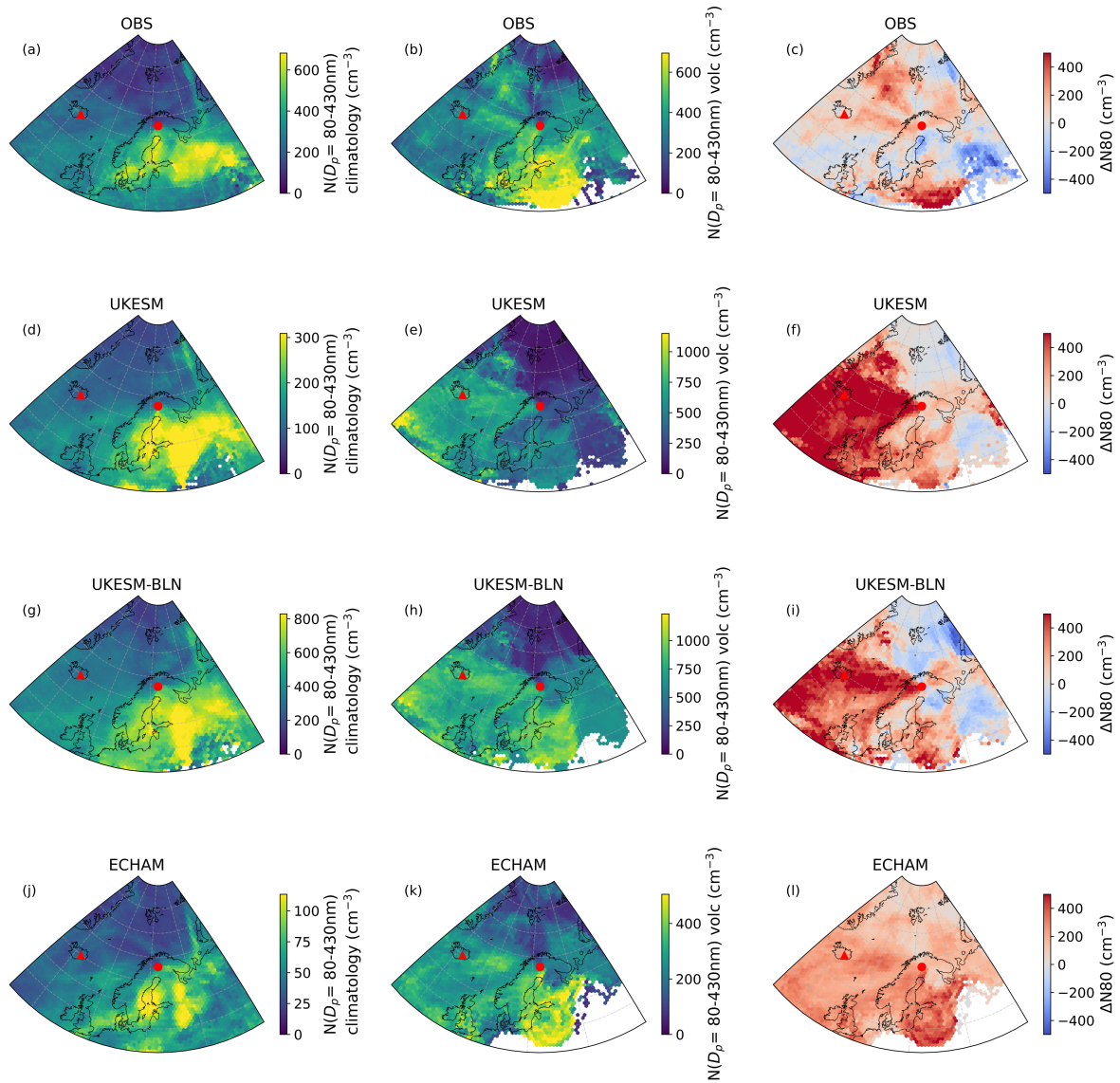


Figure S11: The mean per grid cell for the concentration of particles for $D_p > 80\text{nm}$ (N80) at Pallas for the climatology (a, d, g and j), volcanic period (b, e, h and k) and the difference (volcanic period minus climatology) in concentration (c, f, i and l), utilising the concentration weighted trajectory model. For DMPS with ERA-Interim (a-c), UKESM1.0 (d-f), UKESM1.0-BLN10 (g-i) and ECHAM6.3-HAM2.3 (j-l). Note the difference in colour scale between subfigures.

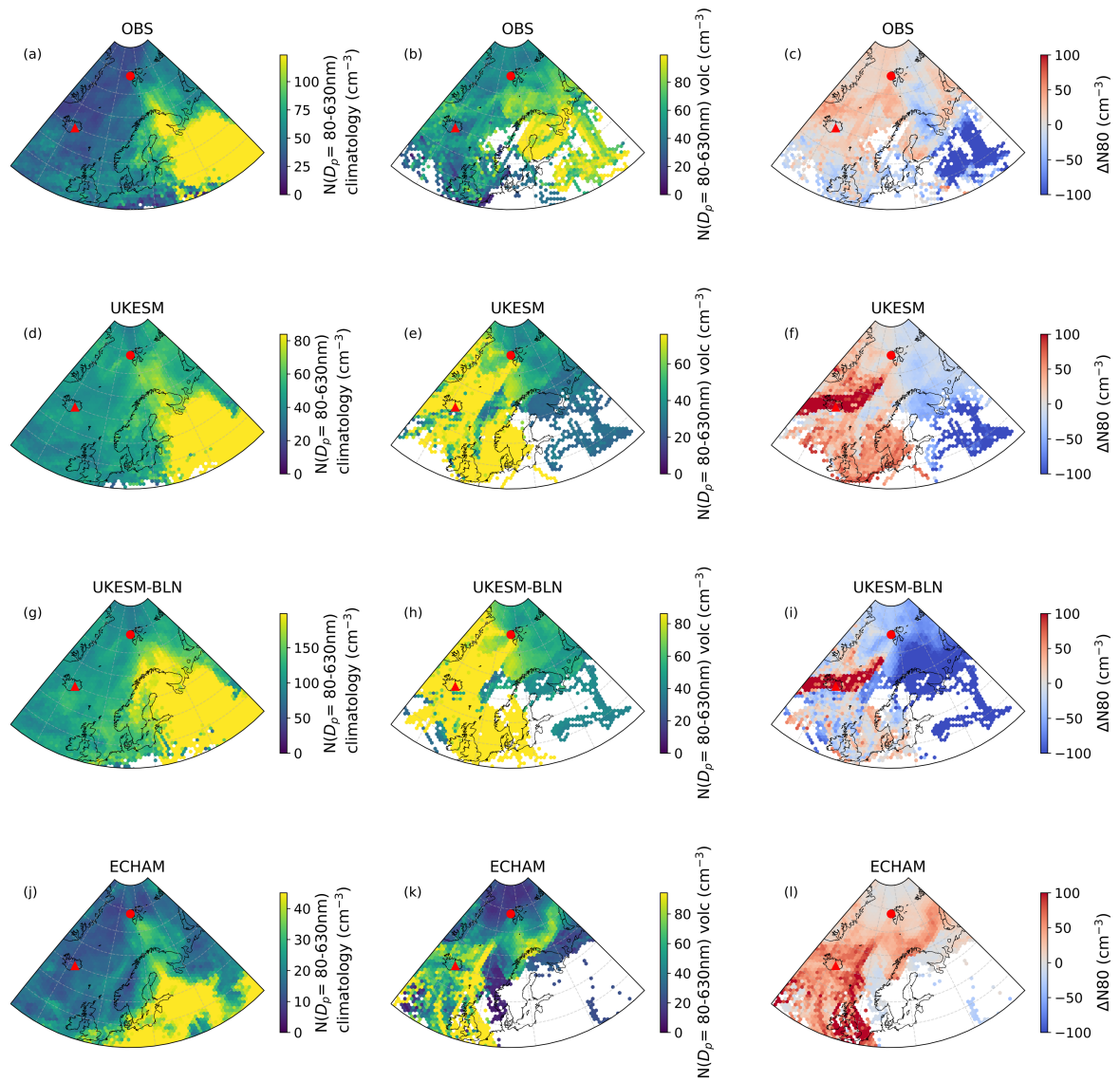


Figure S12: The mean per grid cell for the concentration of particles for $D_p > 80\text{nm}$ (N80) at Zeppelin for the climatology (a, d, g and j), volcanic period (b, e, h and k) and the difference (volcanic period minus climatology) in concentration (c, f, i and l), utilising the concentration weighted trajectory model. For DMPS with ERA-Interim (a-c), UKESM1.0 (d-f), UKESM1.0-BLN10 (g-i) and ECHAM6.3-HAM2.3 (j-l). Note the difference in colour scale between subfigures.